


Tumor-associated neutrophils and macrophages exacerbate antidrug IgG-mediated anaphylactic reaction against an immune checkpoint inhibitor

Takahiro Arai,¹ Tomomi Kokubo,¹ Ruiheng Tang,^{1,2} Hirohito Abo,³ Ayu Terui,¹ Jotaro Hirakawa,³ Hidetaka Akita,⁴ Hiroto Kawashima,³ Akihiro Hisaka,¹ Hiroto Hatakeyama ^{1,2}

To cite: Arai T, Kokubo T, Tang R, *et al.* Tumor-associated neutrophils and macrophages exacerbate antidrug IgG-mediated anaphylactic reaction against an immune checkpoint inhibitor. *Journal for ImmunoTherapy of Cancer* 2022;**10**:e005657. doi:10.1136/jitc-2022-005657

► Additional supplemental material is published online only. To view, please visit the journal online (<http://dx.doi.org/10.1136/jitc-2022-005657>).

TA and TK contributed equally.
Accepted 06 December 2022

ABSTRACT

Background With the increased use of immune checkpoint inhibitors (ICIs), side effects and toxicity are a great concern. Anaphylaxis has been identified as a potential adverse event induced by ICIs. Anaphylaxis is a life-threatening medical emergency. However, the mechanisms and factors that can potentially influence the incidence and severity of anaphylaxis in patients with cancer remain unclear.

Methods Healthy, murine colon 26, CT26, breast 4T1, EMT6, and renal RENCA tumor-bearing mice were treated with an anti-PD-L1 antibody (clone 10F.9G2). Symptoms of anaphylaxis were evaluated along with body temperature and mortality. The amounts of antidrug antibody and platelet-activating factor (PAF) in the blood were quantified via ELISA and liquid chromatography-mass spectrometry (LC-MS/MS). Immune cells were analyzed and isolated using a flow cytometer and magnetic-activated cell sorting, respectively.

Results Repeated administration of the anti-PD-L1 antibody 10F.9G2 to tumor-bearing mice caused fatal anaphylaxis, depending on the type of tumor model. After administration, antidrug immunoglobulin G (IgG), but not IgE antibodies, were produced, and PAF was released as a chemical mediator during anaphylaxis, indicating that anaphylaxis was caused by an IgG-dependent pathway. Anaphylaxis induced by 10F.9G2 was treated with a PAF receptor antagonist. We identified that neutrophils and macrophages were PAF-producing effector cells during anaphylaxis, and the tumor-bearing models with increased numbers of neutrophils and macrophages showed lethal anaphylaxis after treatment with 10F.9G2. Depletion of both neutrophils and macrophages using clodronate liposomes prevented anaphylaxis in tumor-bearing mice.

Conclusions Thus, increased numbers of neutrophils and macrophages associated with cancer progression may be risk factors for anaphylaxis. These findings may provide useful insights into the mechanism of anaphylaxis following the administration of immune checkpoint inhibitors in human subjects.

INTRODUCTION

Anaphylaxis is an immune-mediated systemic acute hypersensitivity reaction that occurs

WHAT IS ALREADY KNOWN ON THIS TOPIC

⇒ Immune checkpoint inhibitor (ICI)-induced toxicity, including immune-related adverse events (irAEs) are of great concern, and anaphylaxis has been identified as a potential adverse event (AE) induced by ICIs. However, the mechanisms underlying anaphylaxis induced by ICIs is poorly understood.

WHAT THIS STUDY ADDS

⇒ Anaphylaxis was caused in an IgG-dependent manner induced by an immune checkpoint inhibitor in tumor-bearing mice, and its severity was exacerbated by tumor-associated neutrophils and macrophages through the release of platelet-activating factor (PAF). Treatment with a PAF receptor antagonist, and depletion of neutrophils and macrophages improved the severity of anaphylaxis.

HOW THIS STUDY MIGHT AFFECT RESEARCH, PRACTICE OR POLICY

⇒ Strategies for the treatment of ICI-induced anaphylaxis are presented. AEs induced by ICIs could be categorized into on-target-dependent autoimmune disease-like symptoms and off-target-dependent symptoms such as anaphylaxis.

rapidly on contact with an allergen in sensitized individuals. Anaphylaxis is classically considered to rely on immunoglobulin E (IgE) antibodies against allergens and antigens.¹ Immune complexes of antigens and IgE against the antigen are recognized by mast cells and basophils via the Fc epsilon receptor 1, followed by massive histamine release. Recently, IgG antibodies were found to trigger IgE-independent anaphylaxis.² Immune complexes of allergen-specific IgG and allergen/antigen activate Fc gamma receptors (FcγRs) and are expressed on myeloid cells, such as macrophages/monocytes,³ basophils,^{4 5} and/or neutrophils,⁶ which in turn release platelet-activating factor



© Author(s) (or their employer(s)) 2022. Re-use permitted under CC BY-NC. No commercial re-use. See rights and permissions. Published by BMJ.

For numbered affiliations see end of article.

Correspondence to

Professor Hiroto Hatakeyama; h-hatakeyama@chiba-u.jp

(PAF) as a chemical mediator. IgG-dependent anaphylaxis may be induced by protein antigens or large molecules such as therapeutic antibodies.^{2,7}

Recently, immune checkpoint inhibitors (ICIs), such as antiprogrammed cell death (aPD-1) monoclonal antibodies (mAbs) and antiprogrammed cell death ligand 1 (aPD-L1) mAbs, have been approved for cancer treatment.⁸ With the increased use of ICIs, side effects and toxicities are of great concern. ICI-induced toxicities mainly include immune-related adverse events (irAEs)⁹ such as colitis, dermatitis, pneumonitis, and hepatitis, indicating the prevalence of off-target effects on an extensively activated immune system. Hypersensitivity reactions and anaphylaxis have also been identified as potential AEs induced by ICIs.¹⁰ Factors that potentially influence the incidence and severity of anaphylaxis in cancer are underexplored. However, a few risk factors and mechanisms have been identified in patients with cancer owing to the rarity of anaphylactic events and their unpredictability.¹¹ Therefore, animal models have provided an understanding of multiple underlying mechanisms.

In this study, we aimed to elucidate the mechanisms by which anaphylaxis was induced by the repeat administration of a PD-L1 mAb and the factors that exacerbated anaphylaxis in tumor-bearing mice. This study provides valuable insights into the mechanisms underlying ICI-induced anaphylaxis in humans.

MATERIALS AND METHODS

Cell culture and tumor inoculation

Murine colon carcinoma CT26 (CRL-2638) and Colon26, breast cancer 4T1 (CRL-2539) and EMT6 (CRL-2755), and renal adenocarcinoma Renca (CRL-2947) cells were obtained from American Type Culture Collection (Manassas, Virginia, USA). BALB/c mice (6 weeks old, female) were purchased from Japan SLC (Shizuoka, Japan). CT26, 4T1, and Renca cells were cultured in RPMI 1640 (Sigma-Aldrich, St. Louis, Missouri, USA) supplemented with 10% fetal bovine serum (FBS; Biowest, Nuaille, France) and 1% penicillin and streptomycin (P/S; Nacalai Tesque, Kyoto, Japan). EMT6 cells were cultured in α -MEM (Nacalai Tesque) supplemented with 10% FBS and 1% P/S. Mycoplasma was not detected in the culture, and the cells were used for experiments within 20 passages after procurement. Cancer cells were subcutaneously transplanted into syngeneic mice using 1.5×10^6 cells in 100 μ L Hanks' balanced salt solution (Gibco, Carlsbad, California, USA).

Treatment of mice with mAbs and chemicals

The antibodies used in this study are listed in online supplemental table S1. Tumor-bearing or healthy mice were randomized and intravenous treated with aPD-1 (RMP1-14), aPD-L1 (10F.9G2 or MIH6), control IgG2a (2A3), or control IgG2b (LTF-2) mAb at a dose of 200 μ g in 100 μ L phosphate-buffered saline (PBS) on days 10, 13, and 17 after tumor inoculation. Tumor-bearing mice

were randomized on day 10 according to tumor volume. Healthy mice were raised for the same period as tumor-bearing mice. The temperature of each animal was measured at baseline and every 5–30 min after the administration of mAbs using a rectal thermometer (AD-1687 and AX-KO4746). Serum was obtained by allowing the blood sample to sit for 30 min at 25°C, followed by centrifugation at 2000 \times g for 10 min at 25°C. For serum transfer, serum (250 μ L/mouse) was intravenously administered to 10F.9G2 naïve CT26 tumor-bearing mice 3 hours before the administration of 10F.9G2. For treatment with epinephrine or CV-6209, CT26 tumor-bearing mice that were treated with 10F.9G2, as mentioned previously, were intraperitoneally (i.p.) treated with epinephrine (6 mg/kg, 100 μ L PBS/mouse) or CV-6209 (150 μ g/100 μ L PBS/mouse) 10 min or 30 min before the third treatment with 10F.9G2 on day 17. To deplete macrophages and neutrophils, CT26 tumor-bearing mice were treated with clodronate liposomes or control liposomes (50 μ L/mouse; Hygieia Bioscience, Osaka, Japan) via i.p. injection on day 16 post-tumor inoculation. To deplete neutrophils, the aGr-1 mAb was intraperitoneally administered to CT26 tumor-bearing mice on days 14, 15, and 16 at doses of 20, 50, and 100 μ g, respectively.

Antidrug antibody (ADA) detection with ELISA

The levels of ADA in the serum with aPD-1 and aPD-L1 mAbs were determined using bridging ELISA. Anti-PD-1 (RMP1-14) and PD-L1 (10F.9G2 and MIH6) mAbs (2 mg/mL) were immobilized on the surface of microplate wells (Nunc-Immuno Plate I, MAXI SORP, Thermo Fisher Scientific, Waltham, Massachusetts) and incubated at 4°C for 16 hours. After washing, the wells were blocked with 3% (w/v) bovine serum albumin (BSA; Nacalai Tesque) in PBS at room temperature for 2 hours. The wells were incubated with serum diluted in 1% BSA in PBS at 25°C for 2 hours. After washing, horseradish peroxidase (HRP)-conjugated goat antimouse IgG (1:4000; BioLegend, San Diego, California, USA) was added to the wells and incubated at room temperature for 1 hour. After washing, 1-step ABTS substrate (Thermo Fisher Scientific) was added to the wells, followed by incubation at room temperature. Reactions were performed with 2 M sulfuric acid, and the OD410 values were evaluated. For antidrug IgE detection, antimouse IgE (2 mg/mL, 1:250, BD Pharmingen, San Diego, California, USA) was immobilized on the surface of the microplate wells, as described previously. After incubation with diluted serum, the wells were incubated with aPD-1 or aPD-L1 mAbs labeled with HRP using EZ-Link Sulfo-NHS-LC-Biotin (Thermo Fisher Scientific). After washing, 1-step Ultra TMB-ELISA substrate (Thermo Fisher Scientific) was added to the wells, and the OD450 values were evaluated as described previously.

Flow cytometry

Splenic single-cell suspensions were prepared by mincing the spleen using a 40 μ m strainer (Grainer,

Frickenhäusen, Germany). The pellet was treated with 1 mL of ACK buffer (pH 7.2, 150 mM NH₄Cl, 10 mM KHCO₃, and 100 μM EDTA), incubated at 25°C for 5 min, and centrifuged at 500×g for 5 min at 4°C. The pellet was washed and resuspended in fluorescence-activated cell sorting (FACS) buffer (0.5% BSA and 0.1% NaN₃ in PBS). Cells were incubated with 10 μg/mL antimouse CD16/32 antibody (BioLegend) in FACS buffer for 10 min at 4°C to block the Fc receptors. After washing the cells with FACS buffer, they were stained with the fluorophore-labeled antibodies listed in online supplemental table S1 for 30 min at 4°C. After washing the cells with FACS buffer, they were stained with 7-AAD (5 μg/mL, BioLegend) for 5 min at 25°C to determine cell viability. The cells were analyzed using a Novocyte Flow Cytometer (ACEA Biosciences, San Diego, California, USA). Data were analyzed using FlowJo software (Tree Star, Ashland, Oregon, USA).

Ex vivo PAF release assay with isolated myeloid cells from the spleen

Neutrophils, macrophages, monocytes, granulocytic myeloid-derived suppressor cells (gMDSCs), and basophils were isolated from the spleens of naïve CT26 tumor-bearing mice on day 17 after tumor inoculation. After immunostaining splenocytes with the APC-labeled anti-Ly6G antibody, Ly6G⁺ and Ly6G⁻ splenocytes were separated using magnetic-activated cell sorting (MACS) with anti-APC magnetic microbeads (Miltenyi Biotec, Bergisch Gladbach, Germany) according to the manufacturer's instructions. Ly6G⁺ cells were immunostained for APC-Ly6C and Ly6G⁺/Ly6C⁺ neutrophils, and Ly6G⁺/Ly6C⁻ gMDSCs were isolated using a cell sorter (SH800S; Sony Biotechnology, Tokyo, Japan). The flow-through containing Ly6G⁻ cells was stained with an APC-labeled anti-Ly6C antibody to separate Ly6C⁺ monocytes and Ly6C⁻ cells using MACS with anti-APC microbeads. The Ly6C⁻ flow-through was stained with an APC-labeled anti-F4/80 antibody to obtain F4/80⁺ macrophages. The F4/80⁻ flow-through was stained with APC-labeled anti-CD49b using MACS with anti-APC microbeads to isolate the CD49⁺ basophils. Serum containing ADA against aPD-L1 mAb was collected from CT26 tumor-bearing mice as described previously. Serum was mixed with 10F.9G2 (final concentration of 10F.9G2 was 0.111 mg/mL) in a total volume of 30 μL. The isolated cells (1.0×10⁶ cells/20 μL) were incubated with the ADA/10F.9G2 mixture for 10 min at 37°C, and 50 μL methanol was added to stop the anaphylactic reaction. Total lipids from the serum were extracted using the Bligh and Dyer method.¹²

Quantification of PAF via LC-MS/MS

PAF was determined using an LC-MS/MS system as described previously.¹³ The LC system consisted of an LC-20AD HPLC system (Shimadzu, Kyoto, Japan) equipped with a CTO-20AC Oven and CBM-20A system control, using a Poroshell 120 HILIC-Z column (100 mm × 2.1 mm, Agilent Technologies, Santa Clara, California,

USA). LC separation was performed using mobile phase A (10 mM ammonium formate in 50% acetonitrile/50% H₂O) and mobile phase B (10 mM ammonium formate in 95% acetonitrile/5% H₂O) at 200 μL/min at 25°C. The separation gradient was as follows: 95% acetonitrile for 10 min, 95%–73% for 10 min, 60% for 3 min, and 95% for 25 min. Mass spectrometry was performed using a QTRAP 4500 LC-MS/MS spectrometer (ABSciex, Framingham, Massachusetts, USA). The MRM mode was used in the positive ion mode and the peak area of the extracted ion chromatogram corresponding to the specific transition for PAF-16 data analysis was performed by using the Analyst V.6.2 software (ABSciex).

Statistical analysis

All data are presented as mean±SE. All in vitro experiments were performed in triplicate. Pair-wise comparisons of subgroups were performed using Student's t-test with Welch's correction. Comparisons between multiple treatments were performed using one-way analysis of variance, followed by an appropriate post hoc test. P values (two-sided) were considered significant at p<0.05. Survival was analyzed using the log-rank test. Statistical analyses were performed using GraphPad Prism 5.0 (San Diego, California, USA).

RESULTS

Lethal anaphylaxis induced by 10F.9G2 depended on the tumor types

Healthy and tumor-bearing mice were intravenously treated with 10F.9G2 (aPD-L1 mAb) on days 10, 13, and 17 post-inoculation (figure 1A). CT26 and 4T1 tumor-bearing mice showed a rapid decrease in body temperature immediately after the third administration of 10F.9G2, with symptoms including loss of spontaneous activity, dyspnea, and piloerection (figure 1B). The maximum temperature drop relative to the baseline (ΔT) in CT26 and 4T1 tumor-bearing mice was approximately 9°C after treatment with 10F.9G2. All CT26 and 4T1 tumor-bearing mice died of adverse events within 40 min (figure 1C). A temperature drop was observed, but 80% of the EMT6 tumor-bearing mice survived. However, healthy mice, and Renca and Colon 26 tumor-bearing mice showed minor or little change in body temperature, with a 100% survival rate. No therapeutic efficacy was observed in all tumor-bearing mice treated with 10F.9G2 (figure 1D). No fatal adverse events were observed in CT26 tumor-bearing mice treated with a different clone of aPD-L1 mAb (MIH6), aPD-1 mAb (RMP1-14), or their isotype controls (online supplemental figure S1).

Next, we evaluated whether the serum of CT26 tumor-bearing mice contained factors capable of triggering the adverse event after treatment with 10F.9G2. On day 17, serum was collected from CT26 tumor-bearing mice treated with 10F.9G2 on days 10 and 13 postinoculation (figure 1E). Treatment of naïve CT26 tumor-bearing mice with 10F.9G2 resulted in fatal anaphylaxis after

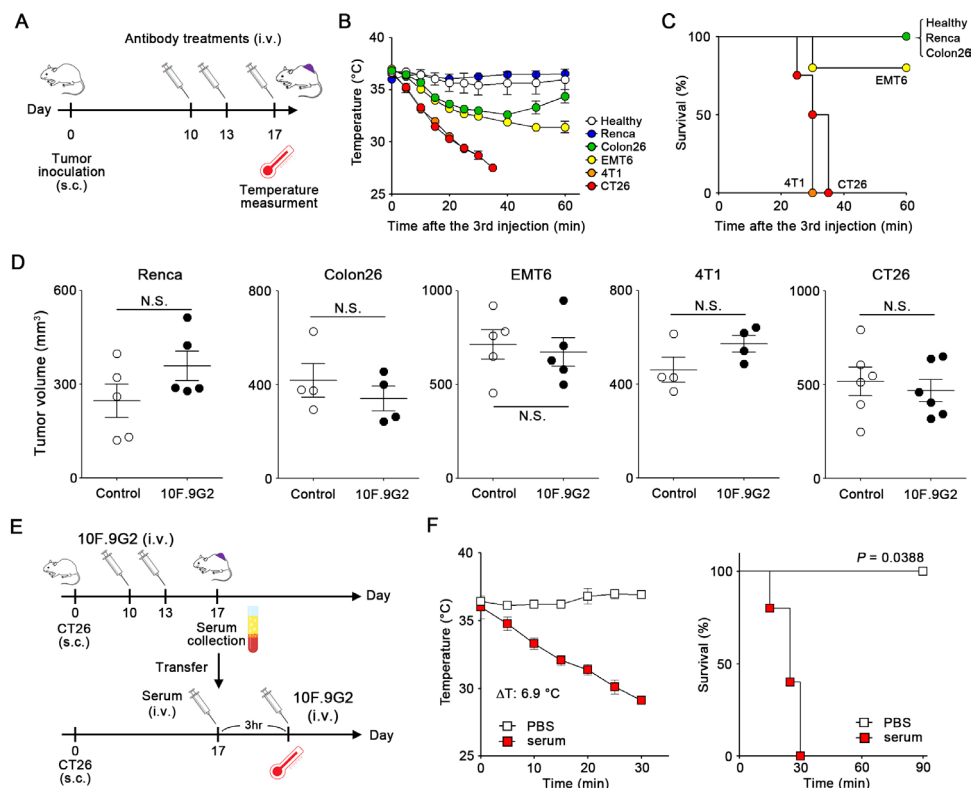


Figure 1 Fatal anaphylaxis induced by sequential treatment with aPD-L1 mAb in CT26 tumor-bearing mice. (A) Experimental schedule for treatment of CT26 tumor-bearing mice with 10F.9G2. (B and C) Body temperature (B) and survival (C) of healthy (n=4), RENCA (n=5), Colon26 (n=4), EMT6 (n=5), 4T1 (n=7), and CT26 (n=11) tumor-bearing mice after the third injection of 10F.9G2. (D) Tumor volume of RENCA (n=5), Colon26 (n=4), EMT6 (n=5), 4T1 (n=4), and CT26 (n=6) tumor-bearing mice on day 17. (E) Experimental schedule for the treatment of CT26 tumor-bearing mice with 10F.9G2 and serum transfer. (F) body temperature and survival rate of CT26 tumor-bearing mice subjected to serum transfer were monitored after the first treatment with 10F.9G2 (n=6). Control mice (n=3) were treated with phosphate-buffered saline (PBS) instead of serum. The maximum temperature drop after treatment with 10F.9G2 is denoted as ΔT . Data are represented as mean \pm SE. N.S., not significant difference.

serum transfer (figure 1F). The results indicated that the lethal adverse event occurred due to a severe anaphylactic reaction to the administered 10F.9G2, and the severity of anaphylaxis depended on the tumor type.

Anaphylaxis caused by PAF via an IgG-mediated pathway

Antidrug IgE antibodies cause anaphylactic reactions to drugs. In addition to the classical IgE-mediated pathway, anaphylaxis in mice is triggered in an IgG-dependent manner.^{11–14} Therefore, we measured antidrug IgE and IgG levels against 10F.9G2 in the serum of healthy and tumor-bearing mice using ELISA. No antidrug IgE was detected in the serum, whereas antidrug IgG was detected in the serum of mice treated with 10F.9G2 (figure 2A). The concentration of antidrug IgG against 10F.9G2 in the serum was proportional to the severity of anaphylaxis (figure 2B). The amount of antidrug IgG against RMP1-14 and MIH6, and their isotype control mAbs in the serum of CT26 tumor-bearing mice was 100-fold lower than that of 10F.9G2 mAb (online supplemental figure S2), which was consistent with the severity of anaphylaxis. The increase in IgG-expressing CD138⁺ plasma cells was observed after treatment of 10F.9G2 (online supplemental figure S3), which indicated that activation and differentiation of B

cells were caused by 10F.9G2, thereby resulting in the production of a large amount of ADA against 10F.9G2. When antidrug IgG complexes stimulate neutrophils, macrophages, and monocytes through their Fc γ receptors, these cells immediately release chemical mediators such as PAFs.^{11–14} Among the mouse IgG isotypes, IgG2a is recognized by mast cells and basophils, which triggers the release of histamine, but not PAF.¹⁵ We analyzed isotypes such as antidrug IgG1 and IgG2a, in the serum of CT26 tumor-bearing mice. The major antidrug IgG isotype produced against 10F.9G2 was IgG1 along with a small amount of IgG2a (figure 2C,D). These results indicated that lethal anaphylaxis may be triggered by the antidrug IgG pathway.

To analyze the anaphylactic pathway, we evaluated whether histamine and/or PAF were released as chemical mediators during anaphylaxis. No obvious changes in histamine levels were detected in the serum of healthy and CT26 tumor-bearing mice when comparing the 10F.9G2 untreated and treated mice (figure 3A). Although histamine-mediated anaphylaxis can be treated with epinephrine,¹⁶ most mice treated with epinephrine died of anaphylaxis (online supplemental figure

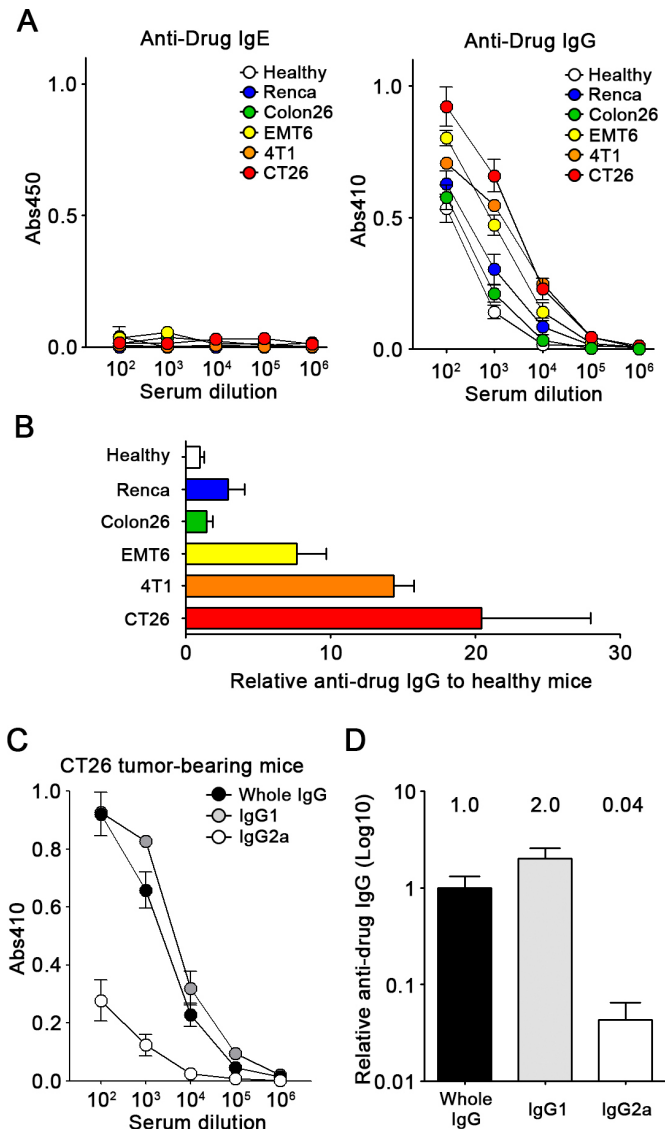


Figure 2 Exploring of subtype of antidrug antibodies to 10F.9G2. (A) Concentrations of the antidrug IgE and IgG against 10F.9G2 in the serum were evaluated using ELISA. healthy mice (n=4), Renca (n=4), EMT6 (n=4), 4T1 (n=9), and CT26 (n=6) tumor-bearing mice were treated with 10F.9G2 on days 10 and 13 postinoculation, and serum was collected on day 17. The x-axis represents the dilution of the serum sample, and the y-axis indicates the absorbance (Abs: A450 or A410). (B) Relative antidrug IgG levels in the serum. The serum dilution ratios resulting in Abs 410 of 0.5 when using antidrug IgG against 10F.9G2 were determined. (C) Evaluation of mouse IgG isotypes in antidrug antibodies using ELISA. CT26 (n=6) tumor-bearing mice were treated with 10F.9G2 on days 10 and 13 postinoculation and serum was collected on day 17. The concentrations of antidrug IgG, IgG1, and IgG2a against 10F.9G2 in the serum were evaluated using ELISA. The x-axis represents the dilution of the serum sample, and the y-axis indicates the absorbance (A410). (D) Relative antidrug IgG levels in the serum. Serum dilution ratios resulting in Abs 410 of 0.2 when using antidrug IgGs against 10F.9G2 were determined. Data are represented as mean±SE.

S4). Thus, anaphylaxis induced by 10F.9G2 was unlikely to result from an IgE-mediated pathway. We quantified the concentration of the chemical mediator PAF in the

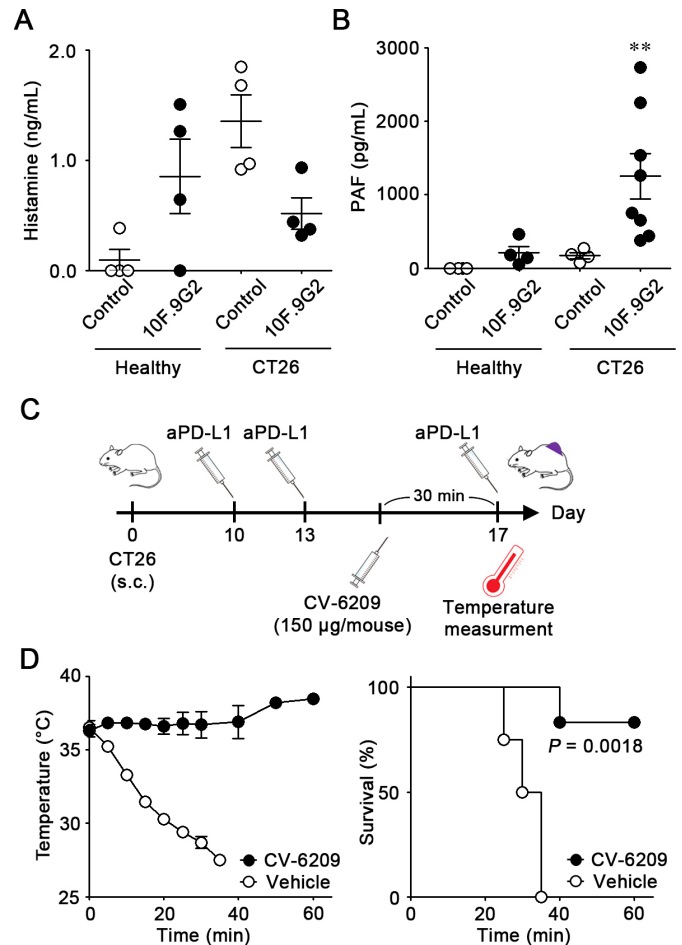


Figure 3 Evaluation of chemical mediators during anaphylaxis after 10F.9G2 administration. (A) Quantification of histamine in the serum by ELISA. Serum was collected 10 min after the third injection of 10F.9G2 from healthy (n=4) and CT26 tumor-bearing mice (n=4) treated with 10F.9G2 on days 10, 13, and 17 postinoculation. Serum from untreated mice was used as control (n=4). (B) Quantification of PAF in the serum by LC-MS/MS. Serum was collected as previously described from healthy (n=4) and CT26 tumor-bearing mice (n=8). **P<0.01. (C) Experimental schedule for the treatment of CT26 tumor-bearing mice with CV-6209 and 10F.9G2. CT26 tumor-bearing mice were treated with 10F.9G2 on days 10 and 13. CV-6209 (150 µg/mouse) was injected intraperitoneally 30 min before the third treatment with 10F.9G2. (D) Body temperature (left) and survival (right) of CT26 tumor-bearing mice treated with vehicle (n=4) or CV-6209 (n=6). Data are represented as mean±SE.

serum using LC-MS/MS (online supplemental figure S5). PAF concentration was significantly elevated in the serum of CT26 tumor-bearing mice during anaphylaxis (figure 3B). We investigated whether treatment with CV-6209,¹⁷ a PAF receptor antagonist, rescued CT26 tumor-bearing mice from anaphylaxis after 10F.9G2 administration (figure 3C). Unlike treatment with epinephrine, treatment with CV-6209 did not result in a decrease in body temperature, and most CT26 tumor-bearing mice survived after 10F.9G2 injection. Therefore, fatal anaphylaxis was prevented by CV-6209 treatment

(figure 3D). These data show that lethal anaphylaxis after 10F.9G2 administration in CT26 tumor-bearing mice occurred in an IgG-dependent manner, followed by the release of PAF as a chemical mediator.

Increased levels of macrophages and neutrophils caused lethal anaphylaxis

Next, we investigated why the amount of PAF was elevated in CT26 tumor-bearing mice compared with that in healthy mice and whether this increase was associated with the varied severity of anaphylaxis against 10F.9G2. Splenomegaly was observed in 4T1 and CT26 tumor-bearing mice (figure 4A), and the spleen is a major clearance organ for 10F.9G2¹⁸; therefore, we focused on alterations in immune cell types in the spleens of mice with different types of tumors. The spleens of healthy mice mainly contained T and B cells, whereas the fraction of these cells decreased in the spleens of CT26 tumor-bearing mice (figure 4B). An increase in the density of CD11b⁺ myeloid cells, especially Ly6G⁺ cells, was observed in the enlarged spleen of CT26-bearing mice compared with that in healthy mice (figure 4C), and the increase in the CD11b⁺ cell fraction was correlated with splenomegaly in tumor-bearing mice (figure 4D). Therefore, CD11b⁺ myeloid cell fractions, including neutrophils, macrophages, monocytes, mast cells, basophils, and gMDSCs in the spleens of tumor-bearing mice were analyzed further (online supplemental figure S6). Along with an increase in CD11b⁺ cells, neutrophil and gMDSC fractions were markedly upregulated in 4T1 and CT26 tumor-bearing mice (figure 4E). In contrast, monocyte and basophil fractions were modestly increased in EMT6, 4T1, and CT26 tumor-bearing mice, and there was no significant change in the fraction of macrophages and mast cells between healthy and tumor-bearing mice. Because of the increased cell number due to splenomegaly, the number of macrophages, neutrophils, gMDSC, and monocytes was increased in the spleen of 4T1 and CT26 tumor-bearing mice (figure 4F).

PAF is released from effector cells such as macrophages, monocytes, basophils, and neutrophils during IgG-dependent anaphylaxis.^{4 6 11 14 19} Since the severity of anaphylaxis was correlated with an increase in myeloid cell numbers, including gMDSCs in the spleen, we hypothesized that these cells are potentially effector cells that release PAF in response to the IgG-mediated reaction, resulting in fatal anaphylaxis in 4T1 and CT26 tumor-bearing mice. Therefore, we investigated cells that were predominantly involved in anaphylaxis. Myeloid cells were isolated from the spleens of CT26 tumor-bearing mice using MACS and a cell sorter (figure 5A). The isolated cells were subsequently incubated with 10F.9G2 and serum containing ADA against 10F.9G2 to enable the cells to release PAF (figure 5B). PAFs were released from neutrophils and macrophages after ex vivo stimulation, whereas little or no PAFs were detected in monocytes, basophils, and gMDSCs (figure 5C). These results suggest that lethal anaphylaxis was caused by PAF released from

neutrophils and macrophages, which increased in CT26 and 4T1 tumor-bearing mice.

We also examined whether depletion of neutrophils and macrophages ameliorated anaphylaxis in vivo. Treatment of CT26 tumor-bearing mice with aGr-1 mAb decreased the number of neutrophils (figure 5D,E). Neutrophil depletion partially rescued CT26 tumor-bearing mice from anaphylaxis induced by 10F.9G2 treatment (figure 5F). Therefore, we attempted to deplete both the cell types. Although clodronate liposomes are known to deplete macrophages, treatment of CT26 tumor-bearing mice with clodronate liposomes depleted both macrophages and neutrophils to the same level as that in healthy mice (figure 5G,H). CT26 tumor-bearing mice showed no or minor anaphylactic symptoms after the depletion of both macrophages and neutrophils (figure 5I). As a result, 80% of the mice survived, with ~1.2°C of ΔT after the third administration of 10F.9G2. These results demonstrated that fatal anaphylaxis in response to 10F.9G2 administration was caused by PAF released from both neutrophils and macrophages in vivo.

DISCUSSION

The preclinical models used in this study showed that repetitive doses of 10F.9G2 induced 100% fatal IgG-dependent anaphylaxis caused by PAF released from neutrophils and macrophages in CT26 and 4T1 tumor-bearing mice. Although epinephrine is the only effective clinical treatment for anaphylaxis, it had only a minor effect on relieving anaphylactic symptoms. However, treatment with the PAF receptor antagonist CV-6209 prevented lethal anaphylaxis in CT26 tumor-bearing mice treated with 10F.9G2. Although no treatment for IgG-mediated anaphylaxis has been established in the clinic, our results suggest that PAF receptor antagonists may be more effective medications for the treatment of IgG-dependent anaphylaxis than epinephrine.

PAF is released from macrophages/monocytes,³ basophils,^{4 5} and/or neutrophils⁶ during IgG-mediated anaphylaxis following the recognition of immune complexes of antigens and antidrug IgG antibodies by Fc γ Rs, particularly Fc γ RIII.¹¹ Our study showed that increased neutrophil and macrophage counts in tumor-bearing mice induced lethal anaphylaxis. Granulocyte colony stimulating factor and granulocyte-macrophage colony stimulating factor, which are highly expressed in CT26 and 4T1 tumors, can accelerate the differentiation and proliferation of myeloid cells.^{20–22} In contrast, monocytes, basophils, and gMDSCs released few or no PAF. The expression profiles of Fc γ Rs may vary among these cell types in mice with cancer. Although the mechanisms by which macrophages and neutrophils respond to immune complexes between 10F.9G2 and ADA remain unknown, an increase in these cells may be a risk factor in cancer patients who exhibit IgG-dependent anaphylaxis against ICIs.

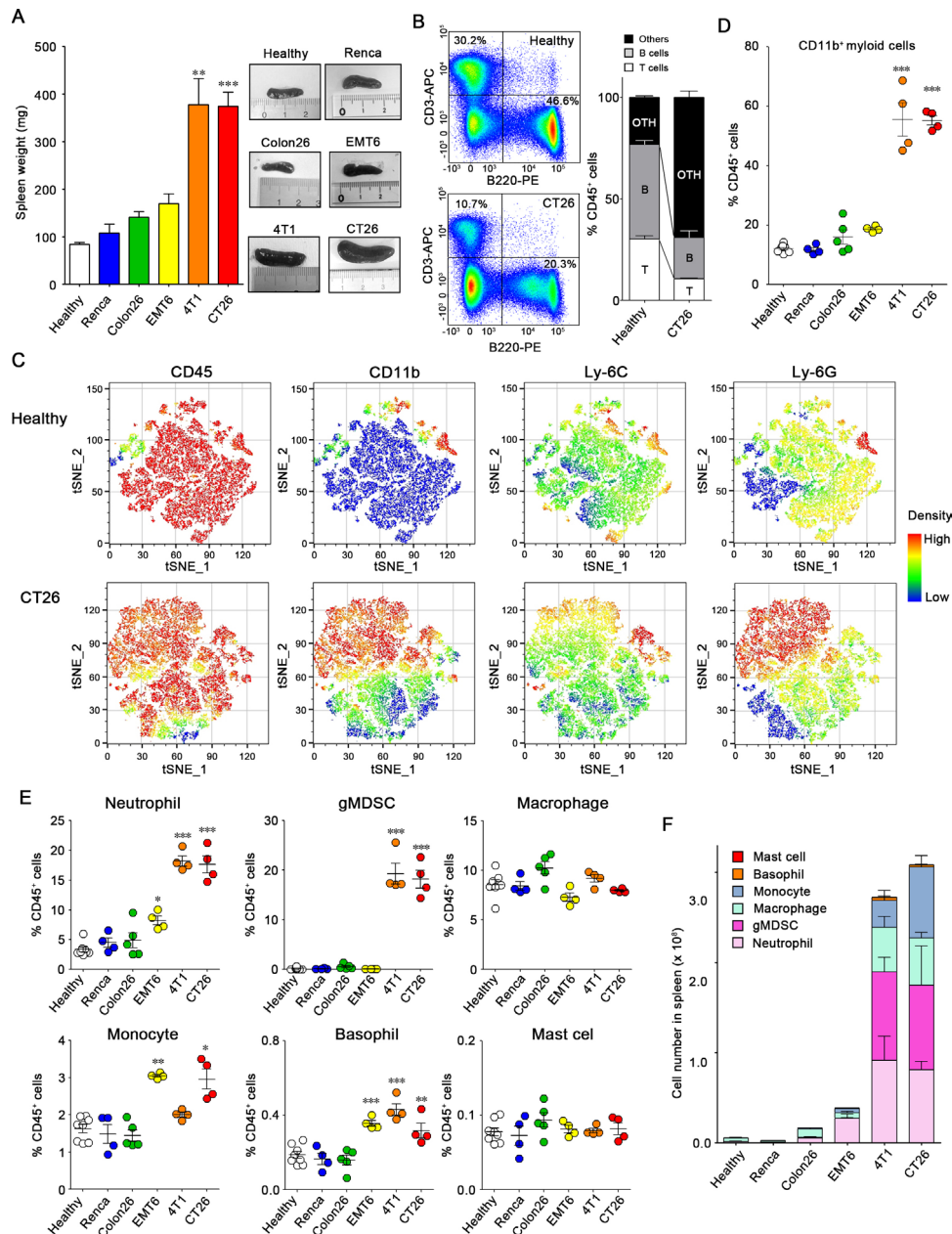


Figure 4 Increase in myeloid cells in the spleen of tumor-bearing mice. (A) Weight (left) and representative images (right) of the spleen from healthy (n=8), Renca (n=4), Colon26 (n=5), EMT6 (n=4), 4T1 (n=4), and CT26 (n=4) tumor-bearing mice on day 17 after inoculation. (B) Left: representative flow plots of CD45⁺ splenocytes from healthy and CT26 tumor-bearing mice stained with anti-CD3 and anti-B220 antibodies. Right: frequency of B cells (CD45⁺B220⁺), T cells (CD45⁺CD3⁺), and other fractions (CD45⁺B220⁻CD3⁻) in the spleens of healthy (n=4) and CT26 tumor-bearing mice (n=4). (C) Representative tSNE plots of splenocytes from healthy and CT26 tumor-bearing mice. tSNE analysis was performed using FlowJo software based on CD45, CD11b, Ly6C, and Ly6G expression. (D) Frequency of CD11b⁺ cells among CD45⁺ splenocytes in the spleens of healthy (n=8), Renca (n=4), Colon26 (n=5), EMT6 (n=4), 4T1 (n=4), and CT26 (n=4) tumor-bearing mice. (E) Frequency of neutrophils (CD11b⁺Ly6C^{int}Ly6G⁺), gMDSCs (CD11b⁺Ly6C⁻Ly6G⁺), macrophages (CD11b⁺Ly6C⁻F4/80⁺), monocytes (CD11b⁺Ly6C⁺Ly6G⁻), basophils (CD49b⁺FcεR1⁺), and mast cells (CD117⁺FcεR1⁺) in splenocytes. (F) Number of neutrophils, gMDSCs, macrophages, monocytes, basophils, and mast cells in the splenocytes. *P<0.05, **p<0.01, ***p<0.001, using one-way analysis of variance followed by Dunnett test (healthy mice vs tumor-bearing mice). Data are represented as mean±SE. gMDSCs, granulocytic myeloid-derived suppressor cells.

The anaphylaxis resulting from 10F.9G2 administration was IgG dependent but not IgE dependent. The potential reasons are as follows: large molecules, such as therapeutic proteins and antibodies, have more potential to induce antidrug IgG antibodies than small

molecular weight drugs.^{2 7} IgG-mediated anaphylaxis requires a much larger dose of antigen than does IgE-mediated anaphylaxis.^{2 11 14 23 24} In this study, the administered dose of 10F.9G2 was approximately 10mg/kg of body weight, which is comparable with the clinical doses

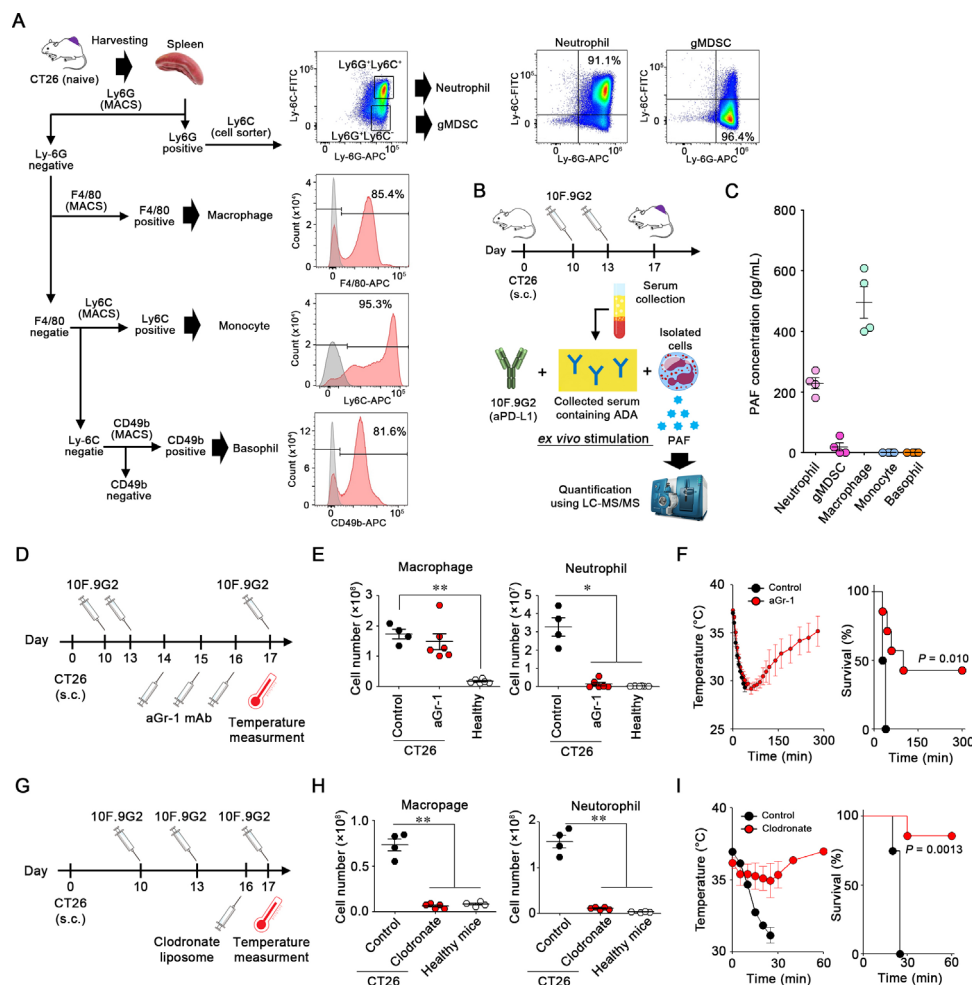


Figure 5 Neutrophils and macrophages cells release PAF during anaphylaxis. (A) Sorting of myeloid cells such as neutrophils, gMDSCs, macrophages, monocytes, and basophils from the spleen via magnetic-activated cell sorting (MACS) and a cell sorter. Histograms represent the purity of each subset. (B) Experimental schedule for ex vivo stimulation of myeloid cells isolated from the spleen of CT26 tumor-bearing mice. (C) The concentration of PAF released from isolated myeloid cells ($n=4$ per sample). (D) Experimental schedule for the treatment of CT26 tumor-bearing mice with 10F.9G2 on days 10, 13, and 17, and aGr-1 mAb on days 14, 15, and 16. (E) Cell numbers of macrophages and neutrophils in the spleen of healthy ($n=6$) and CT26 tumor-bearing mice 24 hours after treatment with either isotype control IgG ($n=4$) or aGr-1 mAb ($n=6$) on days 14, 15, and 16. (F) Body temperature (left) and survival (right) of CT26-tumor-bearing mice treated with either control IgG ($n=4$) or aGr-1 mAb ($n=7$) were monitored on day 17 after the third treatment with 10F.9G2. (G) Experimental schedule for the treatment of CT26 tumor-bearing mice with clodronate liposomes and 10F.9G2. (H) Cell numbers of macrophages and neutrophils in the spleen of healthy ($n=4$) and CT26 tumor-bearing mice 24 hours after treatment with either control ($n=4$) or clodronate ($n=5$) liposomes on day 16. (I) The body temperature (left) and survival (right) of CT26 tumor-bearing mice treated with either control ($n=4$) or clodronate ($n=5$) liposomes on day 16 were monitored after the third treatment with 10F.9G2 on day 17. Data represent mean \pm SE. * $P<0.05$, ** $p<0.01$, *** $p<0.001$ by one-way analysis of variance followed by Bonferroni test. gMDSCs, granulocytic myeloid-derived suppressor cells; PAF, platelet-activating factor.

of aPD-L1 mAbs such as atezolizumab, avelumab, and durvalumab.^{18,25} Clinical doses of aPD-1 mAbs are approximately one-fourth lower, which may induce a lower incidence of anaphylactic reactions toward aPD-L1 mAbs than against aPD-L1 mAbs. In contrast, irAEs induced by aPD-L1 mAbs were of a lower grade and less frequent than those induced by aPD-1 mAbs.²⁶ In general, irAE-like autoimmune diseases induced by ICI occur in patients who respond to ICI via activated T cells.⁹ In this study, 10F.9G2 did not suppress the growth of CT26 and 4T1 tumors (figure 1D). Therefore, anaphylaxis induced by 10F.9G2 may be independent of the typical irAEs induced

by ICIs, and side effects induced by ICIs can be categorized as on-target-dependent and on-target-independent adverse events.

The production of antidrug IgG antibodies against 10F.9G2 depends on the tumor type. We previously reported that 10F.9G2 accumulates in the spleen and is subsequently degraded.¹⁸ Since the spleens of CT26 and 4T1 tumor-bearing mice were enlarged, it is likely that more 10F.9G2 accumulated in the spleens of CT26 and 4T1 tumor-bearing mice, resulting in 10F.9G2 being more exposed as an antigen after degradation. MDSCs reportedly induce Th2 polarization, promote proliferation,

and inhibit apoptosis of B cells^{27–32}; thus, the increased number of gMDSCs in 4T1 and CT26 tumor-bearing mice may stimulate the production of antidrug IgG antibodies. Because fatal anaphylaxis was observed only with administration of 10F.9G2, one particular aPD-L1 mAb, this might not be a general phenomenon related to ICI-mediated adverse events. This phenotype may also depend on the antibody isotype, as repeated doses of 10F.9G2 (aPD-L1 mAb, rat IgG2b) induced the production of large amounts of ADA, whereas MIH6 (aPD-L1 mAb, rat IgG2a) did not. Because rat IgG2b antibodies are recognized by mouse FcγRs,^{33–34} 10F.9G2 binds to PD-L1⁺ cells and FcγR-expressing cells such as macrophages, which may accelerate degradation and antigen presentation. Because the isotype control IgG2b did not result in ADA production, we hypothesized that ADA production in response to 10F.9G2 may require binding to both PD-L1 and FcγR. ADA can induce infusion-related reactions or alter the pharmacokinetics of an agent by affecting its clearance.³⁵ In addition, ADA may decrease treatment efficacy by neutralizing drug activity.³⁶ Therefore, in the future, it is necessary to uncover the mechanisms by which the production of antidrug IgG antibodies varies depending on the type of tumor and isotype.

CONCLUSION

We demonstrated the association of increased neutrophils and macrophages with cancer progression and the release of PAF during IgG-mediated anaphylaxis against anti-PD-L1 mAb. Anaphylaxis was treated with a PAF receptor antagonist. Increases in neutrophil and macrophage counts can serve as markers for patients with cancer who may experience IgG-dependent anaphylaxis in response to ICI treatment.

Author affiliations

¹Lratory of Clinical Pharmacology and Pharmacometrics, Graduate School of Pharmaceutical Sciences, Chiba University, Chiba, Japan

²Laboratory of DDS Design and Drug Disposition, Graduate School of Pharmaceutical Sciences, Chiba University, Chiba, Japan

³Laboratory of Microbiology and Immunology, Graduate School of Pharmaceutical Sciences, Chiba University, Chiba, Japan

⁴Laboratory of DDS Design and Drug Disposition, Graduate School of Pharmaceutical Sciences, Tohoku University, Sendai, Japan

Acknowledgements We would like to thank Editage (www.editage.com) for English language editing.

Contributors Concept and design: AH and HH; development of methodology: TA, TK, HAB, and JH; acquisition of data: TA, TK, RT, HAB, and AT; analysis and interpretation of data: TA, TK, RT and HAB; writing and review: TA, TK, HAB, HA, HK, AH and HH; administrative, technical, or material support: HAB and JH; study supervision: HA, HK, and AH.

Funding The Program for Dissemination of the Tenure-Track system in Japan funded by the Ministry of Education, Culture, Sports, Science, and Technology (MEXT) of Japan, JSPS KAKENHI of Research Activity Start-up (16H06671), Transformative Research Areas (A) 'Material Symbiosis' (21H05506), Takeda Science Foundation, the Inohana Foundation (Chiba University), the Ichiro Kanehara Foundation, and the Research Foundation for Pharmaceutical Sciences (to HH).

Competing interests None declared.

Patient consent for publication Not applicable.

Ethics approval Not applicable.

Provenance and peer review Not commissioned; externally peer reviewed.

Data availability statement Data are available on reasonable request.

Supplemental material This content has been supplied by the author(s). It has not been vetted by BMJ Publishing Group Limited (BMJ) and may not have been peer-reviewed. Any opinions or recommendations discussed are solely those of the author(s) and are not endorsed by BMJ. BMJ disclaims all liability and responsibility arising from any reliance placed on the content. Where the content includes any translated material, BMJ does not warrant the accuracy and reliability of the translations (including but not limited to local regulations, clinical guidelines, terminology, drug names and drug dosages), and is not responsible for any error and/or omissions arising from translation and adaptation or otherwise.

Open access This is an open access article distributed in accordance with the Creative Commons Attribution Non Commercial (CC BY-NC 4.0) license, which permits others to distribute, remix, adapt, build upon this work non-commercially, and license their derivative works on different terms, provided the original work is properly cited, appropriate credit is given, any changes made indicated, and the use is non-commercial. See <http://creativecommons.org/licenses/by-nc/4.0/>.

ORCID iD

Hiroto Hatakeyama <http://orcid.org/0000-0003-3899-0508>

REFERENCES

- Kemp SF, Lockey RF. Anaphylaxis: a review of causes and mechanisms. *J Allergy Clin Immunol* 2002;110:341–8.
- Finkelman FD, Khodoun MV, Strait R. Human IgE-independent systemic anaphylaxis. *J Allergy Clin Immunol* 2016;137:1674–80.
- Jiao D, Liu Y, Lu X, *et al*. Macrophages are the dominant effector cells responsible for IgG-mediated passive systemic anaphylaxis challenged by natural protein antigen in BALB/c and C57BL/6 mice. *Cell Immunol* 2014;289:97–105.
- Tsujimura Y, Obata K, Mukai K, *et al*. Basophils play a pivotal role in immunoglobulin-G-mediated but not immunoglobulin-E-mediated systemic anaphylaxis. *Immunity* 2008;28:581–9.
- Murphy JT, Burey AP, Beebe AM, *et al*. Anaphylaxis caused by repetitive doses of a GITR agonist monoclonal antibody in mice. *Blood* 2014;123:2172–80.
- Jönsson F, Mancardi DA, Kita Y, *et al*. Mouse and human neutrophils induce anaphylaxis. *J Clin Invest* 2011;121:1484–96.
- Steenholdt C, Svenson M, Bendtzen K, *et al*. Acute and delayed hypersensitivity reactions to infliximab and adalimumab in a patient with Crohn's disease. *J Crohns Colitis* 2012;6:108–11.
- Tang J, Yu JX, Hubbard-Lucey VM, *et al*. Trial watch: the clinical trial landscape for PD1/PDL1 immune checkpoint inhibitors. *Nat Rev Drug Discov* 2018;17:854–5.
- Martins F, Sofiya L, Sykiotis GP, *et al*. Adverse effects of immune-checkpoint inhibitors: epidemiology, management and surveillance. *Nat Rev Clin Oncol* 2019;16:563–80.
- Labella M, Castells M. Hypersensitivity reactions and anaphylaxis to checkpoint inhibitor-monoclonal antibodies and desensitization. *Ann Allergy Asthma Immunol* 2021;126:623–9.
- Reber LL, Hernandez JD, Galli SJ. The pathophysiology of anaphylaxis. *J Allergy Clin Immunol* 2017;140:335–48.
- Bligh EG, Dyer WJ. A rapid method of total lipid extraction and purification. *Can J Biochem Physiol* 1959;37:911–7.
- Kim SJ, Back SH, Koh JM, *et al*. Quantitative determination of major platelet activating factors from human plasma. *Anal Bioanal Chem* 2014;406:3111–8.
- Finkelman FD. Anaphylaxis: lessons from mouse models. *J Allergy Clin Immunol* 2007;120:506–15. quiz 516–7.
- Beutier H, Gillis CM, Iannascoli B, *et al*. IgG subclasses determine pathways of anaphylaxis in mice. *J Allergy Clin Immunol* 2017;139:269–80.
- Cardona V, Ansotegui IJ, Ebisawa M, *et al*. World allergy organization anaphylaxis guidance 2020. *World Allergy Organ J* 2020;13:100472.
- Terashita Z, Imura Y, Takatani M, *et al*. CV-6209, a highly potent antagonist of platelet activating factor in vitro and in vivo. *J Pharmacol Exp Ther* 1987;242:263–8.
- Kurino T, Matsuda R, Terui A, *et al*. Poor outcome with anti-programmed death-ligand 1 (PD-L1) antibody due to poor pharmacokinetic properties in PD-1/PD-L1 blockade-sensitive mouse models. *J Immunother Cancer* 2020;8:e000400.



- 19 Muñoz-Cano R, Picado C, Valero A, *et al.* Mechanisms of anaphylaxis beyond IgE. *J Investig Allergol Clin Immunol* 2016;26:73–82. quiz 2p following 3.
- 20 Urduingio RG, Fernandez AF, Moncada-Pazos A, *et al.* Immune-dependent and independent antitumor activity of GM-CSF aberrantly expressed by mouse and human colorectal tumors. *Cancer Res* 2013;73:395–405.
- 21 Carvalho Érika, Hugo de Almeida V, Rondon AMR, *et al.* Protease-Activated receptor 2 (PAR2) upregulates granulocyte colony stimulating factor (G-CSF) expression in breast cancer cells. *Biochem Biophys Res Commun* 2018;504:270–6.
- 22 Yoshimura T, Nakamura K, Li C, *et al.* Cancer cell-derived granulocyte-macrophage colony-stimulating factor is dispensable for the progression of 4T1 murine breast cancer. *Int J Mol Sci* 2019;20:6342.
- 23 Strait RT, Morris SC, Finkelman FD. IgG-blocking antibodies inhibit IgE-mediated anaphylaxis in vivo through both antigen interception and Fc gamma R11b cross-linking. *J Clin Invest* 2006;116:833–41.
- 24 Khodoun MV, Strait R, Armstrong L, *et al.* Identification of markers that distinguish IgE- from IgG-mediated anaphylaxis. *Proc Natl Acad Sci U S A* 2011;108:12413–8.
- 25 De Sousa Linhares A, Battin C, Jutz S, *et al.* Therapeutic PD-L1 antibodies are more effective than PD-1 antibodies in blocking PD-1/PD-L1 signaling. *Sci Rep* 2019;9:11472.
- 26 Sonpavde GP, Grivas P, Lin Y, *et al.* Immune-related adverse events with PD-1 versus PD-L1 inhibitors: a meta-analysis of 8730 patients from clinical trials. *Future Oncol* 2021;17:2545–58.
- 27 Delano MJ, Scumpia PO, Weinstein JS, *et al.* MyD88-dependent expansion of an immature GR-1(+)CD11b(+) population induces T cell suppression and Th2 polarization in sepsis. *J Exp Med* 2007;204:1463–74.
- 28 Sinha P, Clements VK, Bunt SK, *et al.* Cross-talk between myeloid-derived suppressor cells and macrophages subverts tumor immunity toward a type 2 response. *J Immunol* 2007;179:977–83.
- 29 Corzo CA, Cotter MJ, Cheng P, *et al.* Mechanism regulating reactive oxygen species in tumor-induced myeloid-derived suppressor cells. *J Immunol* 2009;182:5693–701.
- 30 Haverkamp JM, Crist SA, Elzey BD, *et al.* In vivo suppressive function of myeloid-derived suppressor cells is limited to the inflammatory site. *Eur J Immunol* 2011;41:749–59.
- 31 Gao J, Wu Y, Su Z, *et al.* Infiltration of alternatively activated macrophages in cancer tissue is associated with MDSC and Th2 polarization in patients with esophageal cancer. *PLoS One* 2014;9:e104453.
- 32 Shen M, Wang J, Yu W, *et al.* A novel MDSC-induced PD⁻¹PD^{L1}⁺ B⁻ cell subset in breast tumor microenvironment possesses immuno-suppressive properties. *Oncimmunology* 2018;7:e1413520.
- 33 Vonderheide RH, Glennie MJ. Agonistic CD40 antibodies and cancer therapy. *Clin Cancer Res* 2013;19:1035–43.
- 34 Dahan R, Segal E, Engelhardt J, *et al.* FcγRs modulate the anti-tumor activity of antibodies targeting the PD-1/PD-L1 axis. *Cancer Cell* 2015;28:285–95.
- 35 Sailstad JM, Amaravadi L, Clements-Egan A, *et al.* A white paper-consensus and recommendations of a global harmonization team on assessing the impact of immunogenicity on pharmacokinetic measurements. *Aaps J* 2014;16:488–98.
- 36 van Brummelen EMJ, Ros W, Wolbink G, *et al.* Antidrug antibody formation in oncology: clinical relevance and challenges. *Oncologist* 2016;21:1260–8.